

# Analyses of high mass resonances at ATLAS and CMS

L. R. Flores Castillo<sup>a</sup>, on behalf of the ATLAS and CMS collaborations

<sup>a</sup>University of Wisconsin-Madison

Several plausible extensions of the Standard Model predict the existence of high mass resonances that can be reconstructed (either fully or partially) in the ATLAS and CMS detectors using leptons, jets and missing transverse energy ( $\cancel{E}_T$ ). We present the results of recent detailed studies of these searches performed by both collaborations, focusing on the potential for discovery and limits setting with an integrated luminosity of the order of 200 pb<sup>-1</sup> per experiment.

## 1. Introduction

Although what is now called the *Standard Model* (SM) of Particle Physics has been extremely successful to predict experimental outcomes, there are several indications that it is not a complete theory of fundamental interactions. Several of the possible extensions of the SM predict narrow states that can be reconstructed (in some cases completely, in others missing one or more neutrinos) using the general-purpose detectors ATLAS and CMS (described in [1] and [2]). Both experimental collaborations have studied their physics reach using these final states.

Here, we report some of the studies and the expected sensitivity of searches for resonances that decay into dileptons, one lepton and a neutrino and leptons plus jets. The results presented correspond to a center of mass energy of 14 TeV. The effect of the lower center of mass energy planned for first data is briefly discussed.

## 2. Detectors

The Large Hadron Collider is scheduled to begin gathering  $pp$  collision data by the end of this year. At the beginning of the data taking period, even with a center-of-mass energy lower than originally planned, it will still produce a large amount of  $W$  and  $Z$  bosons, as well as  $t\bar{t}$  events. As an illustration of the rate, one can point out that the number of  $W$  and  $Z$  bosons contained in 200 pb<sup>-1</sup> of 14 TeV LHC data is expected to be roughly comparable to that of the *full dataset* accumu-

Identifying	Jet rejection	Efficiency
Photons	few $\times 10^3$	80%
Electrons	$\sim 10^5$	60%
B-jets	$\sim 100$	60%
$\tau \rightarrow$ hadrons	few hundreds	50%

Table 1

Expected jet rejections and identification efficiencies at the LHC detectors.

lated by the Tevatron so far. Consequently, these and other similar SM samples are expected to help establish a good understanding of the detector systems relatively soon after startup.

The reconstruction performance of the ATLAS and CMS detectors (described in detail in [3] and [4]) is briefly summarized in table 2 as a function of the total energy  $E$  or the transverse momentum  $p_T$  of the corresponding object. Both detectors have at their disposal silicon-based tracking systems, electromagnetic and hadronic calorimeters (based on very different technologies) and muon spectrometer systems; together, these systems provide powerful identification capabilities (similar for both detectors), summarized in table 1, as well as missing transverse momentum ( $\cancel{E}_T$ ) and jet reconstruction.

## 3. Dilepton searches

### 3.1. Signature, selection

In several models beyond the Standard Model (BSM), dilepton ( $\ell^+\ell^-$ ) decays would provide striking evidence of new high mass resonances



	ATLAS	CMS
Tracker	Si pixels, strips + TRT (pid) $\sigma/p_T \approx 5 \times 10^{-4} p_T \oplus 0.01$	Si pixels, strips $\sigma/p_T \approx 1.5 \times 10^{-4} p_T \oplus 0.005$
EM calorimeter	Lead and liquid Argon (LAr) $\sigma/E \approx 10\%/\sqrt{E} \oplus 0.007$	PbWO <sub>4</sub> crystals $\sigma/E \approx 2 - 5\%/\sqrt{E} \oplus 0.005$
Hadronic calorimeter	Fe+scintillator / Cu+LAr $\sigma/E \approx 50\%/\sqrt{E} \oplus 0.03$	Cu + scintillator $\sigma/E \approx 100\%/\sqrt{E} \oplus 0.05$
Combined muons	2% at 50 GeV to 10% at 1TeV	1% at 50 GeV to 5% at 1TeV

Table 2

Expected reconstruction performance of some detector subsystems of the ATLAS and CMS experiments.

in a relatively clean search. Both detectors have good mass resolutions that should be able to reconstruct these objects even if their daughter particles' momenta were on the order of 1 TeV. On top of that, these signatures would be simple to trigger on. These searches look for two well reconstructed leptons of the same flavor and opposite charges, both with  $|\eta| < 2.5$  (where  $\eta$  is the *pseudorapidity* of the lepton; for electrons, CMS cuts at 2.4 instead) and  $p_T > 30$  or 50 GeV (CMS, ATLAS, respectively). No requirement is imposed in the dilepton opening angle. Given the large rejection factors that both experiments expect against reducible backgrounds (*i.e.*, those composed of combinations of fake and true leptons from SM processes), the main background for this type of search is expected to be the Drell-Yan production. Figure 1 [3] shows the differential cross section, as a function of the dielectron invariant mass, for several SM processes; these estimates were obtained from generator-level quantities, applying rejection factors of  $4 \times 10^3$  and 10 against jets and photons, respectively, and basic kinematic cuts. The neutral Drell-Yan process is dominant, with each of the remaining processes being smaller than 25% of it (and their sum not exceeding  $\sim 30\%$  of the Drell-Yan effective cross section). Figure 2 shows a similar study done using full detector simulation [5], including a signal of  $Z'$ -type boson with a mass of 1 TeV.

Several possible extensions of the SM contain a high-mass gauge boson that can decay into lepton pairs (reference [3] summarizes some of them). In what follows, we will refer to the ‘‘SSM’’ model (in which  $Z'$  couplings are the same as those of the SM  $Z$  boson), unless otherwise noted.

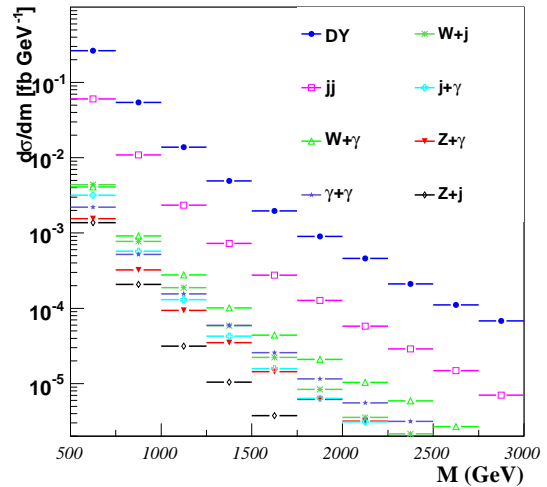


Figure 1. Dielectron invariant mass spectra of SM backgrounds after selection requirements.

### 3.2. Background estimation

Since detector effects and theoretical uncertainties can affect the Monte Carlo -based background estimation, both collaborations are developing control sample strategies to help constrain some of the expected backgrounds. Figure 3 [5] shows, for example, an estimation of the  $t\bar{t}$  background (black triangles) done by measuring the  $b$ -tagging efficiency and then comparing the yields of events with one or two  $b$ -tag(s) to determine the overall  $t\bar{t}$  normalization. The solid yellow histogram shows the actual  $t\bar{t}$  level (from Monte Carlo), which is well in agreement with the estimation. Error bars correspond to the expected statistics after an integrated luminosity of  $100 \text{ pb}^{-1}$ .

It is also possible to estimate the level of the

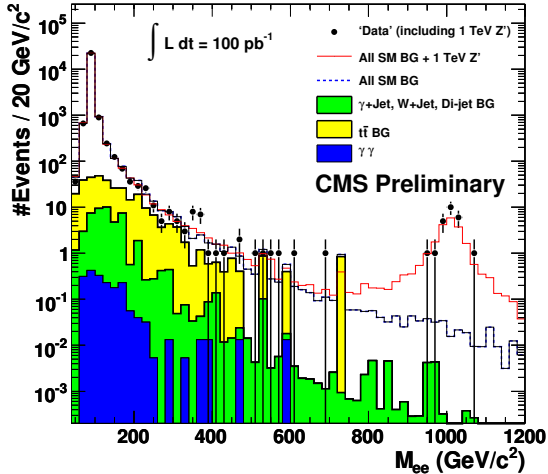


Figure 2. Dielectron invariant mass spectra for  $100 \text{ pb}^{-1}$  for a 1 TeV signal and SM backgrounds.

$t\bar{t}$  background from the number of electron-muon events, since they can be expected to be twice as many as the dimuon events (from this process). In figure 4, the  $t\bar{t}$  spectrum determined using this method (black triangles) is compared with the Monte Carlo  $t\bar{t} \rightarrow ee$  distribution (solid yellow histogram), showing good agreement [5].

### 3.3. Systematic uncertainties

The effects of several sources of systematic uncertainty have been evaluated using full simulation samples; among them, those associated with lepton identification efficiency, momentum or energy scales, momentum resolution, luminosity and the alignment of the muon system, which turns out to be the dominant source. Figure 5 shows the effect of plausible misalignment scenarios on the reconstructed width of potential  $Z'$  signals in CMS [6]; similarly, figure 6 shows the expected increase in the amount of integrated luminosity needed to reach a  $5\sigma$  statistical significance (horizontal line) when such misalignments are introduced in the simulation [3]; the more conservative misalignment scenario would roughly double the amount of luminosity needed to establish a signal.

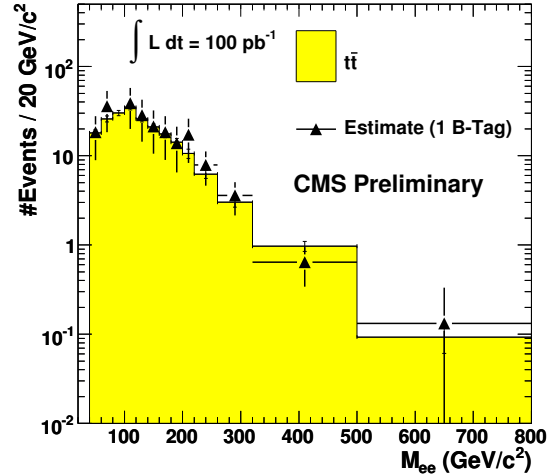


Figure 3. Estimation of the  $t\bar{t}$  background using b-tags (triangles), and from Monte Carlo truth (filled histogram).

### 3.4. Physics reach

The discovery potential has been estimated using several methods, all with compatible results. In one of them, the generator-level shape of the dilepton invariant mass distribution was modeled with a four-parameter family of curves; these parameters describe the mass and the width of the  $Z'$  resonance, its amplitude and the size of its interference with the tail of the SM  $Z$  boson. Detector resolution, acceptance effects and selection efficiencies were obtained from full simulation samples, and applied to these shapes. Figure 7 [3] shows, overlaid, the model obtained by this procedure (solid red line), and the distribution obtained from full simulation (black histogram). From these models, the expected sensitivity is obtained through the use of the log-likelihood ratio (LLR) estimator, in which the *Background Only* (null hypothesis, H0) distribution is compared with the *Signal+Background* (H1) distribution to compute the probability that, when no signal is present, an outcome will have a peak at least as large as the expected signal. This is done by comparing the expected distribution of the LLR for each hypothesis (H0 and H1, as illustrated in figure 8 [3]). Using this procedure, there is no need to restrict the analysis to a mass

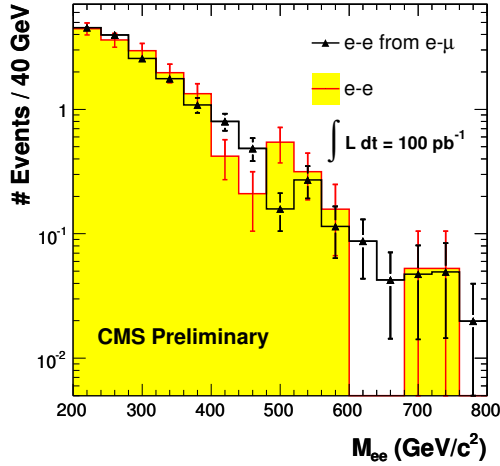


Figure 4.  $t\bar{t}$  background estimation from  $e\mu$  combinations (triangles); histogram: MC truth.

window (and, consequently, neither to determine the optimal size of such window).

Both experiments have comparable physics reach in these searches. Figure 9 shows the expected luminosity needed for to reach a statistical significance of  $5\sigma$  for several  $Z'$  models [3]. If such a state exists slightly above the current Tevatron limits (1 TeV [7]), as low as  $100 \text{ pb}^{-1}$  of integrated luminosity could yield a  $5\sigma$  discovery even in for the least favorable model considered ( $Z'_\psi$ ).

Both collaborations have assessed the effect of lowering the center of mass energy; in particular, when going from 14 to 10 TeV; the production cross-sections for signal and backgrounds are reduced by factors of 2 or 3 (for masses of the  $Z'$  boson between 1 and 2 TeV); accordingly, the luminosity needed for discovery roughly doubles [8].

Besides  $Z'$  models, the physics reach for other possible extensions of the SM has also been evaluated. The sensitivity of a dimuon search for the Graviton in Randall-Sundrum models is illustrated in figure 10 [4]; the sensitivity to the lowest mass states of *technicolor* models is shown in figure 11 [3]; the observation of the latter could require less than  $1 \text{ fb}^{-1}$  of data; the solid line includes the expected effect of the early alignment.

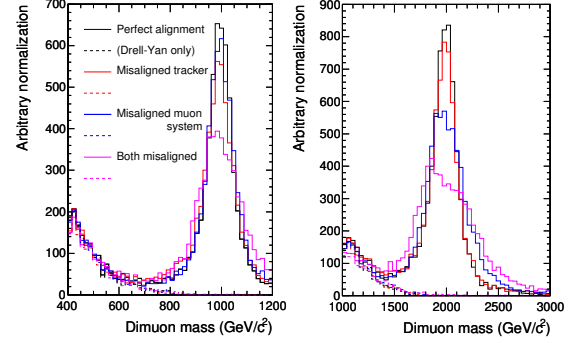


Figure 5. Effect of the muon system alignment uncertainty on the resolution of a dimuon resonance in CMS.

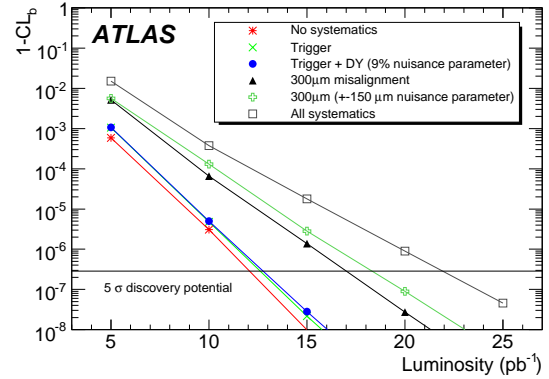


Figure 6. Effect of the alignment uncertainty on the sensitivity of the dimuon search in ATLAS.

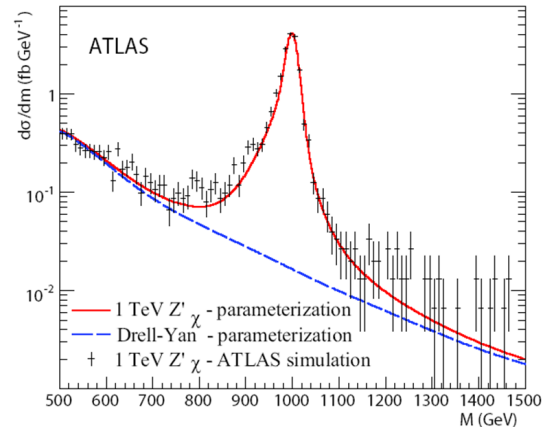


Figure 7. Invariant mass spectrum for a 1 TeV  $Z'_\chi \rightarrow e^+e^-$  obtained with ATLAS full simulation (histogram) and the model described (solid line).

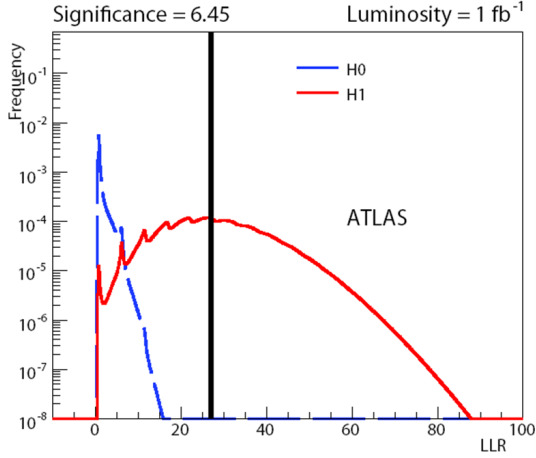


Figure 8. Likelihood ratio distributions for events coming from a background-only sample (H0) and a signal+background sample (H1). The vertical line indicates the median of the H1 distribution; the significance is obtained from the area of the H0 distribution that falls to the right of this line (using the inverse error function).

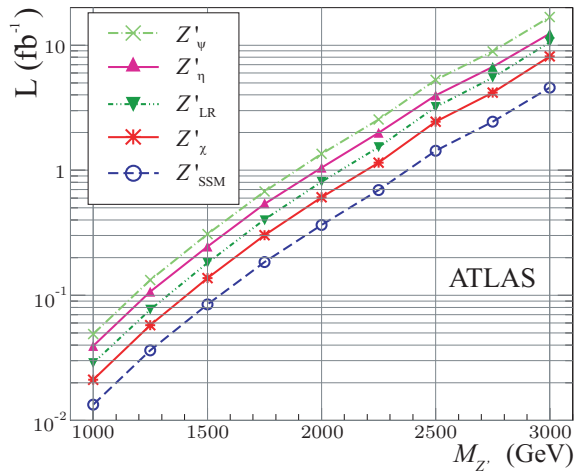


Figure 9. Expected luminosity needed for a  $5\sigma$  discovery for several models of the  $Z'$  boson, as a function of the  $Z'$  mass.

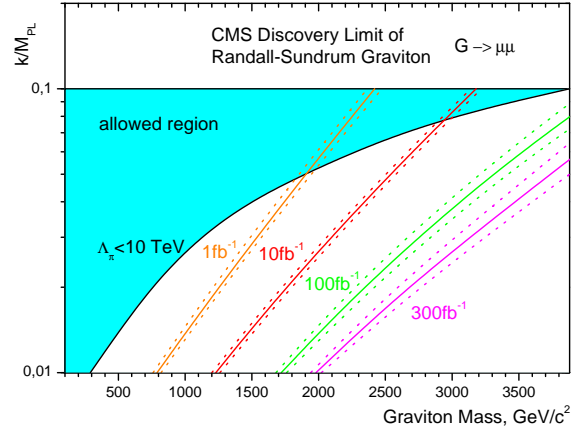


Figure 10. Discovery reach of the dimuon search for Randall-Sundrum gravitons as a function of the coupling  $k/M_{PL}$  and the graviton mass. For each luminosity value shown, the expected significance exceeds  $5\sigma$  in the region to the left of the corresponding curve. Dotted curves show expected variations due to systematic uncertainties.

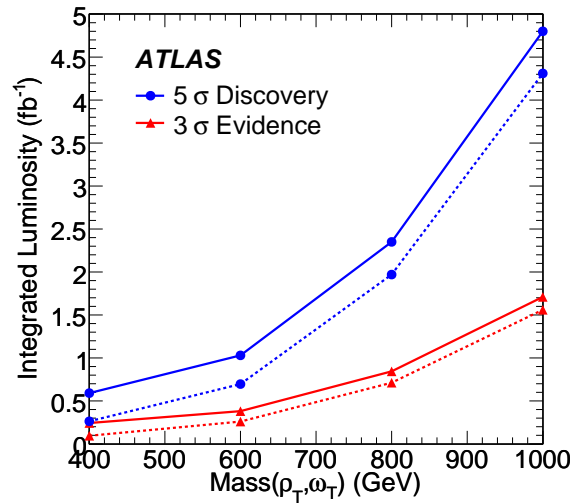


Figure 11. Expected physics reach of a dimuon search for technicolor particles  $\rho_T, \omega_T$ . Dashed lines include only statistical uncertainties; solid lines contain also the systematic uncertainties.

#### 4. Tau pairs

High mass resonances could also decay into pairs of tau leptons, each of which, in turn, can decay hadronically or leptonically. All decay modes (lepton-hadron, hadron-hadron, lepton-lepton) have been studied and used in a combined search. Event selection is based on missing energy cuts, an upper bound on the transverse mass and the scalar sum of the transverse momentum of potential decay products, and a b-jet veto.

Although neutrinos are always present in these decays, the *collinear approximation* (i.e., assuming that the final state leptons have the same direction that their parent tau leptons) allows a good reconstruction of the resonance's invariant mass; figure 12 shows the expected distribution of the reconstructed mass for a  $Z'_{SSM}$  after  $1.0 \text{ fb}^{-1}$  of data, along with the main backgrounds for this type of search [3].

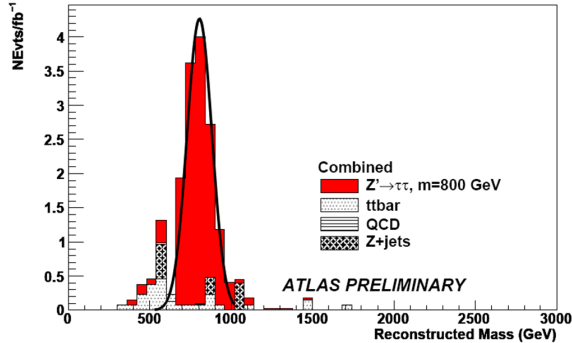


Figure 12. Reconstructed mass distributions, for all  $\tau\tau$  final states and  $m(Z') = 800 \text{ GeV}$ , for  $1 \text{ fb}^{-1}$  of data, using the collinear approximation.

However, when the visible leptons are back-to-back, the above approximation breaks down; in such cases (which are far more frequent), the *visible mass*, defined as the invariant mass of the (four-) vector sum of the momenta of the identified visible decay products of the two taus and the missing transverse momentum, provides a good discriminator for this search. Figure 13 shows the visible mass distribution for signal and back-

grounds [3]. Although the signal-to-noise ratio is much smaller in this case (than when the collinear approximation can be applied), the number of events used is much larger. Figure 14 shows the integrated luminosity needed for 3 and  $5\sigma$  evidence using a combination of these two methods, and of all decay channels [3]. A  $Z'_{SSM}$  with a mass up to  $1.2 \text{ TeV}$  could yield a  $5\sigma$  significance with about  $1 \text{ fb}^{-1}$  of data.

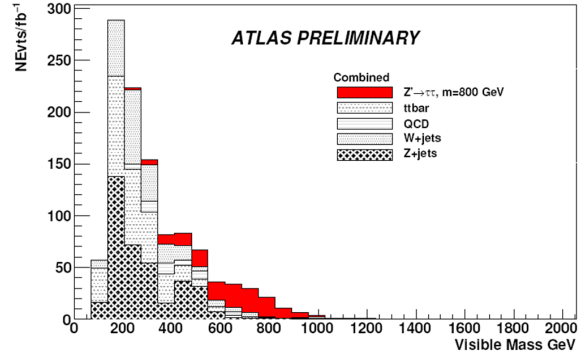


Figure 13. Visible mass distributions obtained from all final states and  $m(Z') = 800 \text{ GeV}$  for  $1 \text{ fb}^{-1}$  of data.

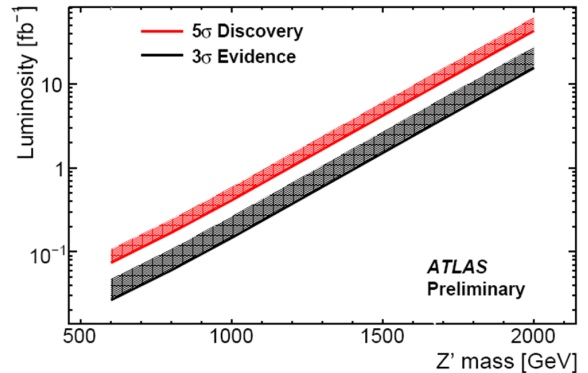


Figure 14. Luminosity required for  $3\sigma$  evidence or  $5\sigma$  discovery (all  $\tau\tau$  channels combined) as a function of the mass of the  $Z'$  resonance, including a 20% systematic uncertainty.

## 5. Lepton-neutrino searches

Several BSM scenarios include heavy charged gauge bosons that are able to decay into a charged lepton plus a neutrino. As in the case of the SM  $W$  boson, the *transverse mass*  $m_T$ , defined as  $\sqrt{2p_T \cancel{E}_T (1 - \cos \Delta\phi(\ell, \cancel{E}_T))}$ , helps extract them.

Events are required to have exactly one, isolated, high- $p_T$  lepton (electron or muon), a large amount of missing transverse energy  $\cancel{E}_T$  (over 50 GeV) and most of their  $\cancel{E}_T$  should come from the lepton and the neutrino (*i.e.*, they should have low jet activity). These cuts are very effective to reduce the dijet and  $t\bar{t}$  backgrounds; after applying them the main remaining background is the off-shell, high- $m_T$  tail of the SM  $W$  boson, which has a falling  $m_T$  distribution, while the expected signal would have a Jacobian edge at the mass of the  $W'$  boson, which can be exploited by keeping only events with  $m_T > 0.7m_{W'}$ . Figure 15 shows the  $m_T$  distribution of three  $m_{W'}$  signals and the backgrounds after all selection criteria (electron channel) [9]; background distributions are stacked; signals are not.

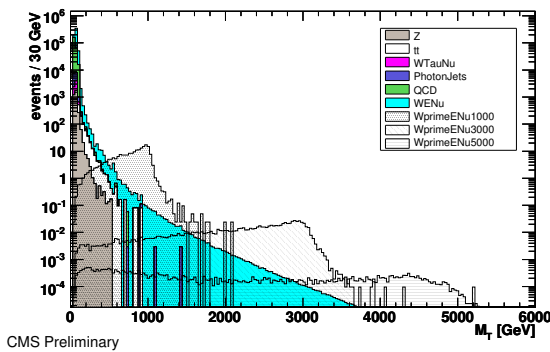


Figure 15. Transverse mass distributions after cuts of signal and SM backgrounds in the  $W'$  search.

Figure 16 [9] shows the expected luminosity needed to reach a  $3\sigma$  and a  $5\sigma$  evidence, as a function of the mass of the  $W'$  boson (using, as a benchmark, the Altarelli model [10]), and the

luminosity needed to set a 95% confidence level exclusion, also as a function of  $m(W')$ . Due to the large production cross section of this model, an integrated luminosity of the order of  $200 \text{ pb}^{-1}$  is expected to allow LHC experiments to probe masses up to about 2.5 TeV, which would be well above the current ( $D\phi$ ) limit of 1 TeV [11].

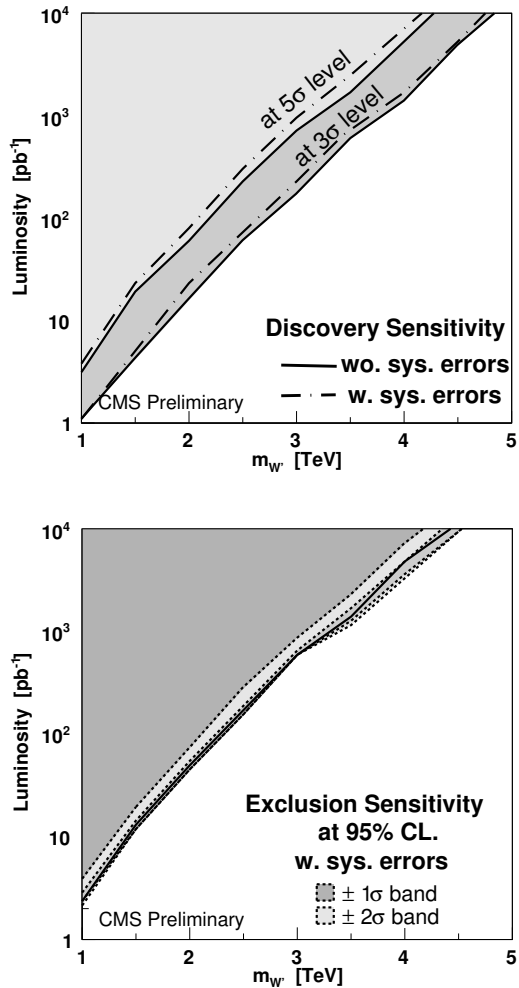


Figure 16. Luminosity needed to establish evidence (top) or to set a 95% CL limit (bottom), as a function of the mass of the  $W'$  boson.

## 6. Leptons plus jets

Final states with two leptons and one or two jets also have a good chance of allowing LHC to improve the current experimental limits at the early stages of data taking. Both leptoquark (LQ) models and Left-Right Symmetric Models (LRSM) produce this signature, and in both cases the background can be reduced strongly.

### 6.1. Leptoquarks

Leptoquarks (LQ) are bosons carrying quark and lepton numbers. Experimental constraints favor three generations of LQ, each coupled to a SM generation. Current experimental limits (from DØ) place the mass of the first-generation LQ over 256 GeV, and that of the second generation LQ above 251 GeV. Figure 17 shows Feynman diagrams for the pair production of LQ, where each of them decays (with branching ratio  $\beta$ ) into a quark and a lepton; for the search, events are required to have 2 leptons of opposite charge and the same flavor and at least two jets. Expected backgrounds (Drell-Yan,  $t\bar{t}$  and diboson production) are rejected by requirements on the transverse momenta of the leptons, the scalar sum of the  $p_T$  of leptons and jets, the dilepton invariant mass and the lepton-jet invariant mass. Figure 18 shows the expected lepton-jet invariant

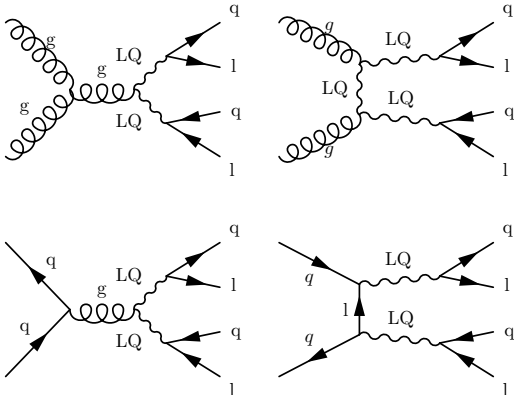


Figure 17. Feynman diagrams for leptoquark pair production.

mass spectrum before and after the above cuts; both correspond to a first generation leptoquark signal, at an integrated luminosity of  $100 \text{ pb}^{-1}$  [3].

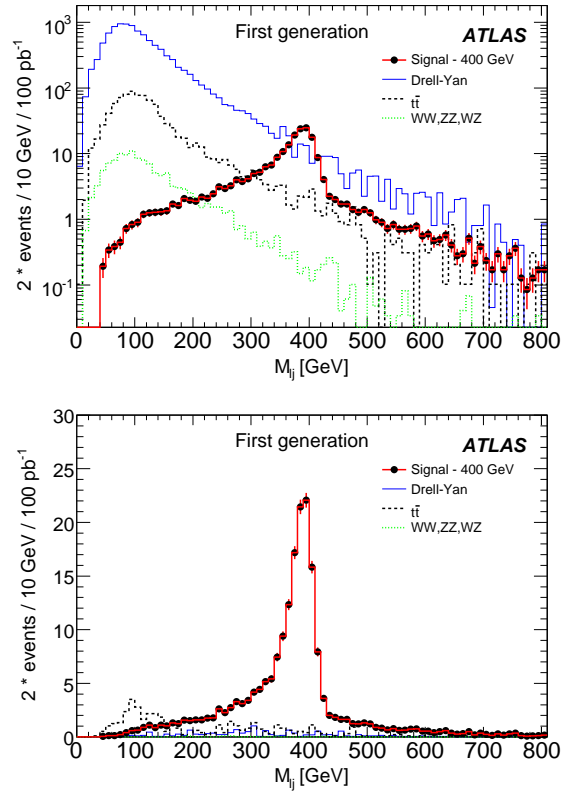


Figure 18. Reconstructed electron-jet invariant mass in the first-generation leptoquark analysis (with  $m_{LQ} = 400 \text{ GeV}$ ) after baseline selection (top) and after all selection criteria (bottom).

Figure 19 shows the  $5\sigma$  contours for the leptoquark search in ATLAS, showing the branching ratio ( $\beta$ ) that would yield a  $5\sigma$  discovery as a function of the total integrated luminosity used, for a 400 GeV leptoquark [3]. For this mass, a value of  $\beta^2$  above 0.3 would allow a  $5\sigma$  signal with less than  $100 \text{ pb}^{-1}$  of data.



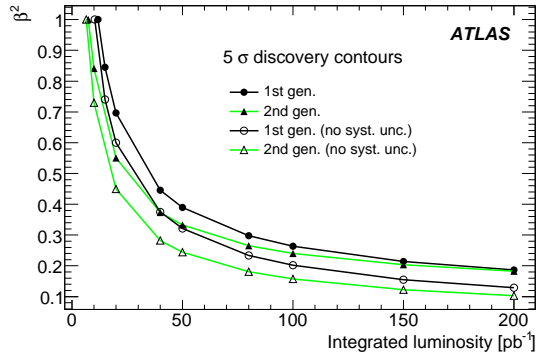


Figure 19.  $5\sigma$  discovery potential for first and second generation scalar leptoquarks (with  $m_{LQ} = 400$  GeV).

## 6.2. Left-right symmetric models

These models, which address the non-zero neutrino mass and baryogenesis, incorporate three heavy right-handed Majorana neutrinos ( $N_e, N_\mu, N_\tau$ ), and some also introduce right-handed heavy bosons ( $W_R$  and  $Z'$ ). Figure 20 shows a possible decay in one such model, where the  $W_R$  boson decays into a lepton and a Majorana neutrino  $N_\ell$ , which ultimately produces a lepton and two jets. Since all final state particles can be reconstructed, it is possible in this model to reconstruct both the  $N_\ell$  and the  $W_R$  masses. Selection cuts similar to those used in the LQ search allow a strong reduction of the expected backgrounds also in this case; figures 21 and 22 show the reconstructed mass of  $N_\ell$  and  $W_R$ , respectively, after cuts, for two possible scenarios: one with  $m_{W_R} = 1.8$  TeV and  $m_{N_e} = m_{N_\mu} = 300$  GeV, denoted as LRSM\_18.3, and one with  $m_{W_R} = 1.5$  TeV and  $m_{N_e} = m_{N_\mu} = 500$  GeV, labeled as LRSM\_15.5 [3].

Figure 23 [3] shows the expected significance of this search for the same scenarios; triangles correspond to LRSM\_18.3, while squares represent LRSM\_15.5. Solid/hollow markers show the significance when systematic uncertainties are included/excluded. As shown, for these mass values, a  $5\sigma$  significance could be reached with less than  $150 \text{ pb}^{-1}$  and  $40 \text{ pb}^{-1}$  of collision data, respectively.

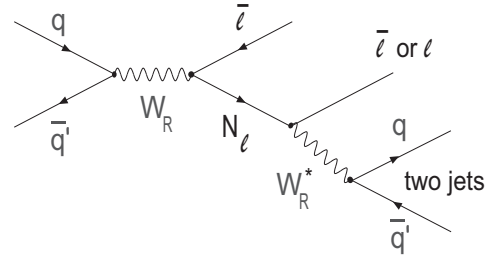


Figure 20. Feynman diagram for  $W_R$  boson production and its decay to a Majorana neutrino  $N_\ell$ .

## 7. Discussion

Several plausible extensions of the SM predict narrow resonances, which can be reconstructed using the ATLAS and CMS general-purpose detectors at LHC. Background estimation procedures, fit-based strategies, and statistical tools have been developed to extract these potential signals from collision data. Studies done for a center-of-mass energy of 14 TeV have shown that several of these models could be established at the  $5\sigma$  level even with  $O(100 \text{ pb}^{-1})$  of integrated luminosity. In some of the models considered, preliminary estimations using a lowered center-of-mass energy of 10 TeV show that the initial run may still be enough to go beyond Tevatron limits.

## REFERENCES

1. ATLAS Collaboration, JINST 3:S08003,2008.
2. CMS Collaboration, JINST 3:S08004,2008.
3. ATLAS Collaboration, CERN-OPEN-2008-20, arXiv:0901.0512 [hep-ex].
4. CMS Collaboration, CERN/LHCC 2006-021, CMS TDR 8.2 (2006)
5. CMS Collaboration, CMS-PAS-EXO-08-001.
6. CMS Collaboration, CMS-PAS-SBM-07-002.
7. CDF Collaboration, arXiv:0811.0053 [hep-ex].
8. CMS Collaboration, CMS PAS EXO-09-006.
9. CMS Collaboration, CMS-PAS-EXO-08-004.
10. G. Altarelli, B. Mele and M. Ruiz-Altaba, Z. Phys. C **45** (1989) 109 [Erratum-ibid. C **47** (1990) 676].

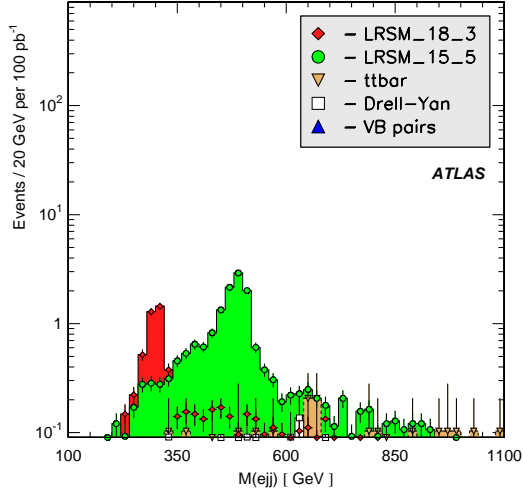


Figure 21. Distribution of reconstructed invariant mass for  $N_e$  candidates in background and signal events after background suppression.

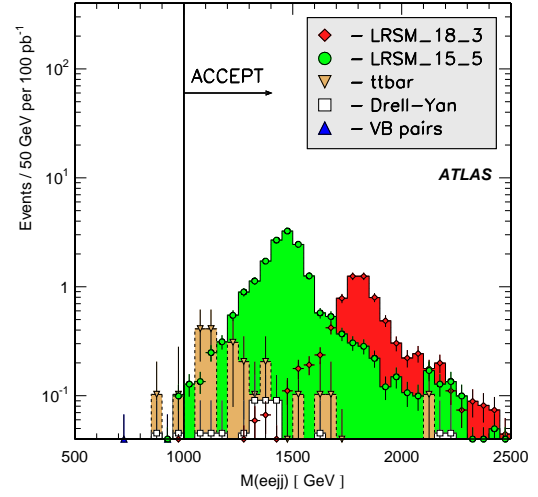


Figure 22. Distribution of reconstructed invariant mass for  $W_R \rightarrow eN_e$  candidates in background and signal events after background suppression.

11. V. M. Abazov *et al.* [D0 Collaboration], Phys. Rev. Lett. **100** (2008) 031804

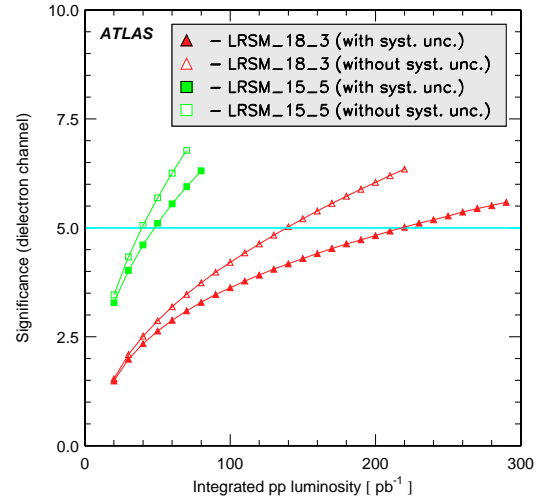


Figure 23. Expected signal significance versus integrated luminosity for two mass hypotheses for the  $N_e$  neutrino and the  $W_R$  boson.